International Journal of Applied Earth Observation and Geoinformation 130 (2024) 103898

Contents lists available at ScienceDirect

International Journal of Applied Earth Observation and Geoinformation

journal homepage: www.elsevier.com/locate/jag

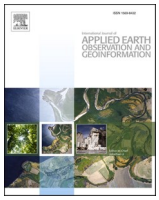

Annual winter crop distribution from MODIS NDVI timeseries to improve yield forecasts for Europe

Lorenzo Seguini [a,*], Anton Vrieling [a], Michele Meroni [b,1], Andrew Nelson [a]

[a] University of Twente, Faculty of Geo-Information Science and Earth Observation (ITC), PO Box 217 7500AE, Enschede, the Netherlands
[b] Seidor Consulting, Barcelona, Spain

ARTICLE INFO

Keywords:
Wheat
GDD
Classification
Crop group
Crop monitoring
Phenology

ABSTRACT

Crop yield forecasts allow policy makers to anticipate market behaviour and regulate prices. Annual updates on which crops are grown where can improve crop yield forecast accuracy. Existing efforts to map crops across the European Union resulted in late-season map availability or short time series that do not meet forecasting requirements. We propose a new approach to retrieve annual winter crop maps and improve forecasting efforts by identifying pixels with dominant winter crop signals using moderate resolution imagery. These pixels are distinguished from summer crop signals based on their senescence date. When this date precedes the theoretical maturity date of a winter crop, expressed in GDD, the pixel is labelled as having a dominant winter crop signal. Our 2018 map accurately identified 77% and 83% of dominantly winter-crop area, when compared to farmers' declaration data and a high-resolution crop map for Europe, respectively. While the resulting annual winter crop maps underestimated winter crop area, derived region-specific annual NDVI profiles better described winter crop phenology as compared to the use of static maps. Regression analysis between these regional NDVI profiles and statistical wheat yield data indicates that our annual maps help explain more yield variability than static maps, with an RMSE reduction of 3% for the EU27 as whole. The proposed approach is applicable to long historical timeseries and provides maps before the end of the agricultural season. Those maps positively impact crop yield description, notably in eastern, northern, and northeastern European regions.

1. Introduction

Crop yield forecasting systems (CYFSs) provide timely yield forecasts to predict crop production. This information helps policy makers to address market distortions from under- or overproduction. CYFSs require environmental timeseries long enough to provide robust correlation with crop yield statistics. Crop yield forecast accuracy relies on accurate information on crop distribution, particularly when remotely-sensed crop health indicators are used as predictors (Zhang et al., 2019). As such, improvements in these underlying data will lead to improvements in CYFS accuracy.

For an operational CYFS, crop maps need to meet four requirements: *i)* a complete spatial coverage; *ii)* a high classification accuracy; *iii)* within-season availability to timely obtain crop growth characteristics; and *iv)* a timeseries long enough to match the time-frame covered by the CYFS. Because crop distribution is not static, annual crop maps are preferable over static maps to effectively link remote sensing signals with the target crop. Three main approaches exist for annual crop mapping: *i)* assembling information from farmers on what is grown where; *ii)* classifying crop types from high-resolution satellite data; and *iii)* classifying dominant crop groups from low-resolution satellite data. We define crop group as crop types with a similar growing season (e.g., winter crop). For each approach we report mainly on EU-focussed studies because of its peculiar agricultural system with advanced agricultural management but relatively small field size compared to other relevant crop producing regions. A further motivation to focus on Europe is our ultimate aim, i.e., to improve the European Commission's CYFS (EC-CYFS). At present, static crop maps are still used in the EC-CYFS (Lecerf et al., 2019) and in crop yield forecasting studies elsewhere (von Bloh et al., 2023; Meroni et al., 2021).

First, annual field-specific information about which crop is cultivated where is collected from farmers throughout the European Union (EU27) and stored in the LPIS (Land Parcel Information System). LPIS is composed of national systems with different information, availability,

* Corresponding author.
E-mail addresses: l.seguini@utwente.nl, lorenzo_seguini@yahoo.it (L. Seguini).
[1] Under contract with the European Commission, JRC, Ispra, Italy

https://doi.org/10.1016/j.jag.2024.103898
Received 4 December 2023; Received in revised form 24 April 2024; Accepted 5 May 2024
Available online 9 May 2024

and time coverage. Efforts to standardize LPIS are still limited (Schneider et al., 2023), new maps are seldomly disclosed before the end of the ongoing season, and time series are short for most countries. As such LPIS does not serve the needs of operational crop yield forecasting at the EU27 scale.

For the second approach, i.e., obtaining crop type maps from high resolution satellite data, presently long timeseries of accurate, crop-specific maps are not freely available for the entire EU27. Outside Europe Landsat imagery was used in combination with *in-situ* data to produce large-scale yearly crop maps based on supervised classification; examples include the Cropland Data Layer in the US, which is available since 2008 (Johnson, 2019), and China- and Australia-wide maps for the years 2012–2015 (Teluguntla et al., 2018). Other Landsat-based studies relied on *in-situ* data to classify summer crop types from temperature and phenological metrics Landsat-based for a county in the US (Zhong et al., 2014), while Tian et al.(2019) found that for north-eastern China the supervised classification of winter crops from the combined NDVI (Normalized Difference Vegetation Index) time series of Sentinel-2 and Landsat outperforms a classification based on a parametric model from NDVI MODIS time series. For individual European countries several efforts have provided single-year or short crop type timeseries through training of classification algorithms with LPIS and high-resolution satellite data (Preidl et al., (2020) and Blickensdörfer et al. (2022) for Germany; Defourny et al. (2019) for Ukraine). d'Andrimont et al. (2021) made the only public crop type map for the whole European Union (EU27). They applied a random forest classifier to multi-temporal S1 data from 2018 and validated the map with LPIS data for the same year. Their reported accuracy ranged from 40 %, at the beginning of the European crop growing season (February), to 83 % at the end (November). All these studies resulted in crop maps for a single year or at best a few recent years as they usually depend on high-resolution imagery with relatively short timeseries. In addition, mapping with high resolution data requires a large amount of training samples, well distributed over the years and among the observed regions, which is very difficult to collect for studies spanning large regions and multiple countries, such as the EU27.

The third approach exploits low-resolution satellites, such as the 250 m-resolution MODIS (Moderate-Resolution Imaging Spectroradiometer), providing timeseries with sufficient length (i.e., about 20 years) to meet the needs for crop yield forecasting. While their use for crop type mapping in areas with large fields is possible (Wardlow et al., 2007) for smaller field sizes, typical of Europe, the crop mix in a pixel makes specific crop type mapping difficult and the focus is moved to crop groups.

Skakun et al. (2017) used a region-specific Gaussian mixture model (GMM) to discriminate winter and summer crops in Ukraine and in Kansas (US) using MODIS NDVI at 250 m spatial resolution and accumulated growing degree days (GDD), for years 2000 to 2014. They expressed the time of NDVI in "thermal time" (i.e., GDD) to reduce its temporal variability from weather, and thus providing a more consistent link with crop phenology (McMaster, 1997). Their assumption is that high NDVI values in springtime are indicative of winter crops, as unlike summer crops, they green up shortly after winter. The GMM was set to fit the histogram of the NDVI frequency, at given time, with a bimodal distribution; labelling the class with larger NDVI mean as winter crop. The annual maps generated for Ukraine attained an accuracy of 94 % for 2013 when compared against field data and explained 76 % of the winter crop area variability obtained from regional statistics. The maps could be produced up to two months before winter crop harvest. For Europe, Weissteiner et al. (2019) used 250 m-resolution MODIS NDVI timeseries to identify arable land pixels with pure winter or summer crop signals. They used a region-specific GMM, similar to Skakun et al. (2017), but labelled the GMM classes according to *a priori* regional agro-statistical knowledge. Winter and summer crops were separated using an empirical threshold on NDVI values (e.g., 0.4 for winter crops). Despite that $>$ 72 % of winter crop pixels were correctly identified, based on LPIS data of one region in Spain, they classified only 11 % of the arable land pixels. The use of these maps improved the R^2 (+0.15 on average) between the yield of the dominant winter crop of a region and NDVI, compared to the use of a static arable land map for 37 % of the considered regions (Ronchetti et al., (2023).

For yield forecasting purposes, the winter crop maps should allow to extract an NDVI signal that effectively represents crop development throughout the season. Because Weissteiner et al. (2019) and Skakun et al. (2017) only consider the green-up phase, this requirement may not be met as the senescence phase is also crucial for yield formation (Porter and Gawith, 1999; Barlow et al., 2015). In fact, focusing on the timing of peak NDVI cannot unequivocally describe the winter crop signal, as confusion may arise with other vegetation peaking in spring. The method of Weissteiner et al. (2019) presents two other limitations: *i)* the classification is only available at the end of the season (e.g., in October), which prevents its use for yield forecasting at the end of the winter crop season in August, and *ii)* in some regions a very low number of pixels is retained, which may not effectively represent regional crop development.

Long timeseries of spatially-explicit crop information are required to obtain better predictors of crop status and hence improve crop yield forecasts for Europe. While MODIS NDVI timeseries provide long timeseries, the existing approaches do not provide maps that guarantee the extraction of representative NDVI profiles that can effectively describe winter crop yield formation. To address this, we focused on three objectives:

1. to develop a method to map winter crop areas using MODIS NDVI timeseries and temperature data;
2. to assess the accuracy and the spatial and temporal consistency of the resulting winter crop maps;
3. to evaluate if the use of our annual winter crop maps improves crop yield forecast accuracy.

2. Materials and methods

2.1. Study area

This study focuses on the EU27, the 27 countries that constitute the European Union in 2023 (Table S1). Winter crops account for approximately 70 % of the EU27 crop area but are often grown in the same region with summer crops and other cover types (e.g., temporary fallow land). For the third objective of this paper, i.e., to assess if crop yield forecasts can be improved using annual winter crop maps, we focus on soft wheat. This is because a compound winter crop yield would lack physical meaning due to the large differences in average yield values between different winter crops. Soft wheat (30 % of total crop area) is widely distributed in the EU27 (Fig. 1) and its regional statistics (i.e., yield, area, production) are complete while most other winter crops have only local presence and discontinuous statistics. Fig. 1 shows the study area and the administrative regions considered, following the Nomenclature of territorial units for statistics of the European Union (NUTS) regions of 2016. The selected NUTS level for each country corresponds to the finest spatial detail of available agricultural statistics (Table S2).

2.2. Data

2.2.1. Input data

To describe the annual crop dynamics, we used a smoothed NDVI timeseries produced with a MODIS processing chain (Klisch and Atzberger, 2016). It ingests 250 m resolution NDVI time series from MODIS Terra and Aqua (8-day composites, MOD09Q1 and MYD09Q1, Collection 6.1) for the whole EU, applies a Whittaker smoothing filter (Eilers, 2003), and resamples the timeseries to a 10-day timestep. We used the resulting 10-day NDVI composites for January 2002 to September 2020.

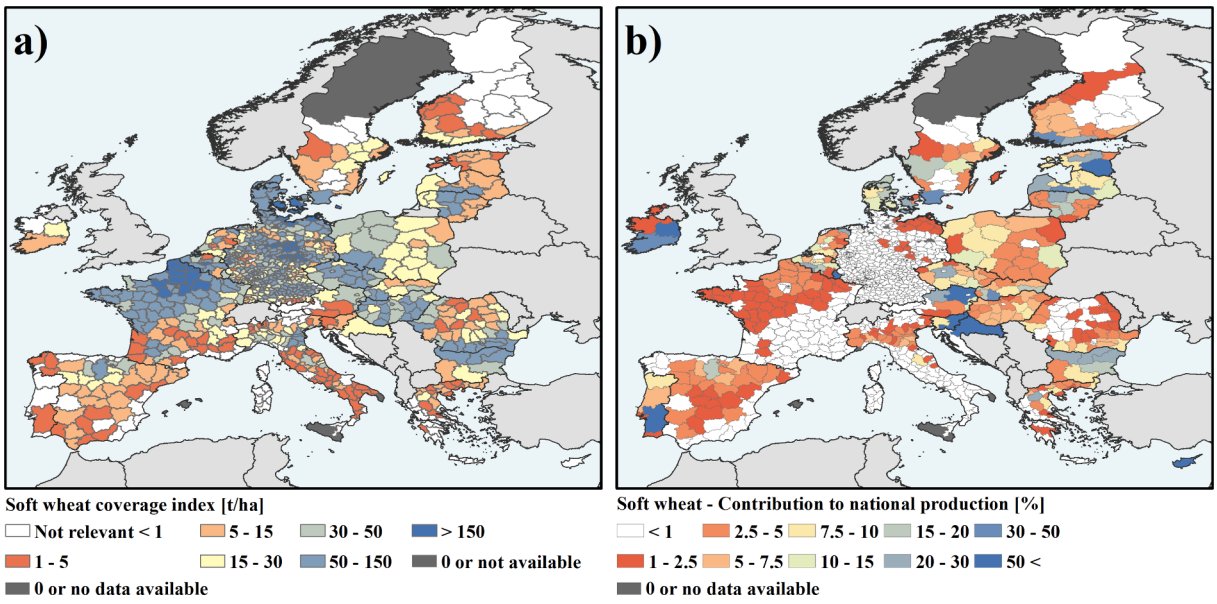

Fig. 1. The study area. Panel a) shows a normalized index (soft wheat coverage index) computed as the ratio between the total soft wheat production (tonnes) and the total land area of the corresponding region, using averaged data for 2002–2020. Panel b) shows the regional share of each administrative region to national production for soft wheat.

We used GDD to compute the annual theoretical maturity date of winter crops. GDD were computed from the daily average temperature data provided by the Gridded Agro-Meteorological Data (GAMD) of the EC-CGMS (Toreti, 2014), covering geographical Europe at a 25 × 25 km spatial resolution. From the daily average temperature we computed the GDD using a base temperature for active crop development of 0 °C (i.e., daily accumulation of average temperature when the average temperature is above 0 °C) starting from 1 January, following Skakun et al. (2017) to 31 August. While winter crop sowing dates may differ by several weeks according to the region or crop considered, their impact on estimated maturity date is small. This is because our GDD accumulation that takes 1 January as the reference may miss out GDD from early sowing (e.g., in October), or add GDD in case of late sowing (e.g., in March). Because the October-March period represents relatively cold periods, the GDD will be small, whereas spring and summer temperatures affect the GDD sum most. For each grid cell, the theoretical maturity date was defined annually as the first day when the GDD sum exceeds 1800. We used winter soft wheat maturity time as proxy for all winter crops since it is one of the winter crops with the longest cycle (NDAWN, 2023). The base temperature and the GDD requirement for winter wheat maturity were based on literature (NDAWN, 2023; IPAS - FAD - USDA, 2023; Knott et al., 2017; Steduto et al., 2012; Porter and Gawith, 1999) and WOFOST-CGMS model parametrization (Ceglar et al., 2019).

2.2.2. Validation and comparison data

Our results were validated against ground truth data and compared against an existing crop-type mapping product. While the validation exercise is limited to a number of countries, the comparison covers the whole EU. For the validation we used LPIS data available for 2018 collected from the CHEAP (Common Harmonized European Agriculture Parcels) dataset (Claverie et al., 2024). The CHEAP dataset collected and homogenized crop distribution at field scale, as from the LPIS, from the EU27 countries that provided these distributions as public data. This information is stored in vector layers representing the field boundaries and the associated crop planted for each year covered by LPIS. The crop nomenclature of the CHEAP dataset is normalised to the EuroCrops legend (Schneider et al., 2023). From the EuroCrops legend we selected a subset of crops matching our definition of winter crop group (Table S4) and extracted the corresponding crop parcels from all the available regions (i.e. Austria, Belgium, Brandenburg (Germany), Denmark, Catalunya (Spain), France, Netherlands, and Portugal). This sample accounts for 27 % of the EU27 arable land. The winter crop polygons were converted into areal fraction images (AFI_{winter_LPIS}) using the 250 × 250 m MODIS grid definitions indicating the share of winter crop in each pixel. Besides the validation using the CHEAP dataset, a comparison was performed against the crop-type map of d'Andrimont et al. (2021) for the year 2018, hereafter referred to as the EU2018 map. This map is considered suitable for the comparison as it covers the full EU and d'Andrimont et al. (2021) reported a high classification accuracy for the winter crop group (84 %) compared against ground data. From EU2018 we computed six AFIs (AFI_{arable_land}, AFI_{winter_crops}, AFI_{soft_wheat}, AFI_{summer_crops}, AFI_{dry_pulses}, and AFI_{fodder_crops}) each representing the share of the considered crop class (Table S4) per pixel. AFI_{arable_land} is the sum of all the other classes with the exception of AFI_{soft_wheat}, which is a subclass of AFI_{winter_crops}. This definition of the arable land class includes only crop types and leaves out other agricultural cover types (e.g., grassland).

Besides the 10 m-resolution crop map for Europe, we further compared our maps against winter crop area statistics. From the APRO_CPSHR database of Eurostat (2023) we obtained winter crop area for each EU27 country and for the EU27 as whole, as crop area statistics for smaller administrative regions are not readily available for all regions and would require substantial harmonization efforts to be presented at the EU27 scale. Further details are provided in Tables S5 and S6. The total winter crop area was calculated as the sum of the area of each winter crop.

To assess if our maps may help to improve yield prediction, we selected regional yield statistics for soft wheat for the EU27 regions (Fig. 1) at the finest spatial detail as from Ronchetti et al. (in preparation). The target time window was 2002 to 2020 to overlap with the used MODIS data. For evaluation purposes, we only retained regions with yield timeseries of 10 or more consecutive years.

2.3. Methods

We aimed to detect MODIS pixels with a predominant presence of winter crops, namely that have a clear senescence before the expected maturity date, hence a significant fraction (>50 % for pixels with 100 % coverage of arable land) of the pixel is expected to have a winter crop in

the considered year. Fig. 2 provides a graphical description of our approach. It consists of three parts: 1) the definition of season boundaries; 2) the definition of maturity at 1800 GDD and 3) the definition of a clear NDVI senescence signal before maturity date. Regarding point 3, we assumed that if an arable pixel has a predominance of winter crops (Fig. 2a and Fig. 2b), its senescence period, characterised by a pronounced NDVI decline, should be observable before the date corresponding to 1800 GDD. On the contrary, if a pixel has no winter crop predominance no senescence should be observable by that date (Fig. 2c and Fig. 2d).

The approach works pixelwise and considers for each season the 10-day MODIS NDVI data between 1 January and 31 August. We applied it to all the pixels where AFI_{arable_land} is at least 1 %. The approach searches for the earliest observation in the timeseries (point M with coordinates $TIME_M$ and $NDVI_M$) satisfying three conditions: 1): $TIME_M$ occurs before the time of 1800 GDD, and after the seasonal NDVI maximum (Max); 2) $NDVI_M$ has a maximum value of 75 % of the NDVI amplitude (i.e., Max – Min in Fig. 2); 3) point M is preceded by a point with a larger NDVI and followed by one with lower NDVI. The pixel is identified as having a dominant winter crop signal if all three conditions are met. The 75 % threshold was determined with a trial-and-error process on a large set of samples. Fig. 2b illustrates that no point would match the three conditions when using either a 25 % or 50 % threshold.

We then applied our approach to every arable land pixel for all years of the timeseries, resulting in annual maps of arable land pixels with a dominant winter crop signal; these pixels may consist of pure winter crop or contain a significant proportion of winter crop (Fig. 2b). From here onward we refer to these maps as AFI_{winter_MODIS}, for which the pixel values remain the areal fractions of the original share of arable land (i.e., as derived from EU2018 based crop map, AFI_{arable_land}).

2.3.1. Consistency analysis

To assess the quality of our AFI_{winter_MODIS} maps we examined their spatial and temporal consistency. The spatial consistency was assessed by comparing our map to the AFI_{winter_LPIS} and AFI_{winter_crops} map derived from the CHEAP dataset and d'Andrimont et al. (2021), all products referring to the year 2018. Using thresholds on winter crop fraction, AFI_{winter_MODIS} was used to derive three maps, AFI_{winter_MODIS}, $AFI_{winter\_MODIS}50$, and $AFI_{winter\_MODIS}90$, including pixels with at least 1 %, 50 %, and 90 % of winter crop coverage, respectively. The same thresholding scheme was applied to AFI_{winter_LPIS} and AFI_{winter_crop}. Errors were then determined for the three thresholds. AFI_{winter_MODIS} was validated against AFI_{winter_LPIS} and compared against AFI_{winter_crop}. In addition, we also compared AFI_{winter_crop} against AFI_{winter_LPIS} to independently assess the accuracy of AFI_{winter_crop} as a reference for the EU27 region. Standard metrics were employed for all the assessments, encompassing commission error (both absolute and relative to classified winter crop), and omission error (both absolute and relative to total winter crop as per the reference map). As accuracy metrics we included producer's and user's accuracy, which quantify correct detections relative to total classified winter crop and to the reference winter crop map, respectively. Additionally, a map of simple difference (AFI_{winter_MODIS} minus AFI_{winter_crop}) was generated to assess how their spatial patterns match. Lastly, to assess the extent to which our MODIS maps erroneously assigned winter crop dominance to non-winter crop pixels we compared AFI_{winter_MODIS} to the reference non-winter maps of $AFI_{summer\_crops}90$.

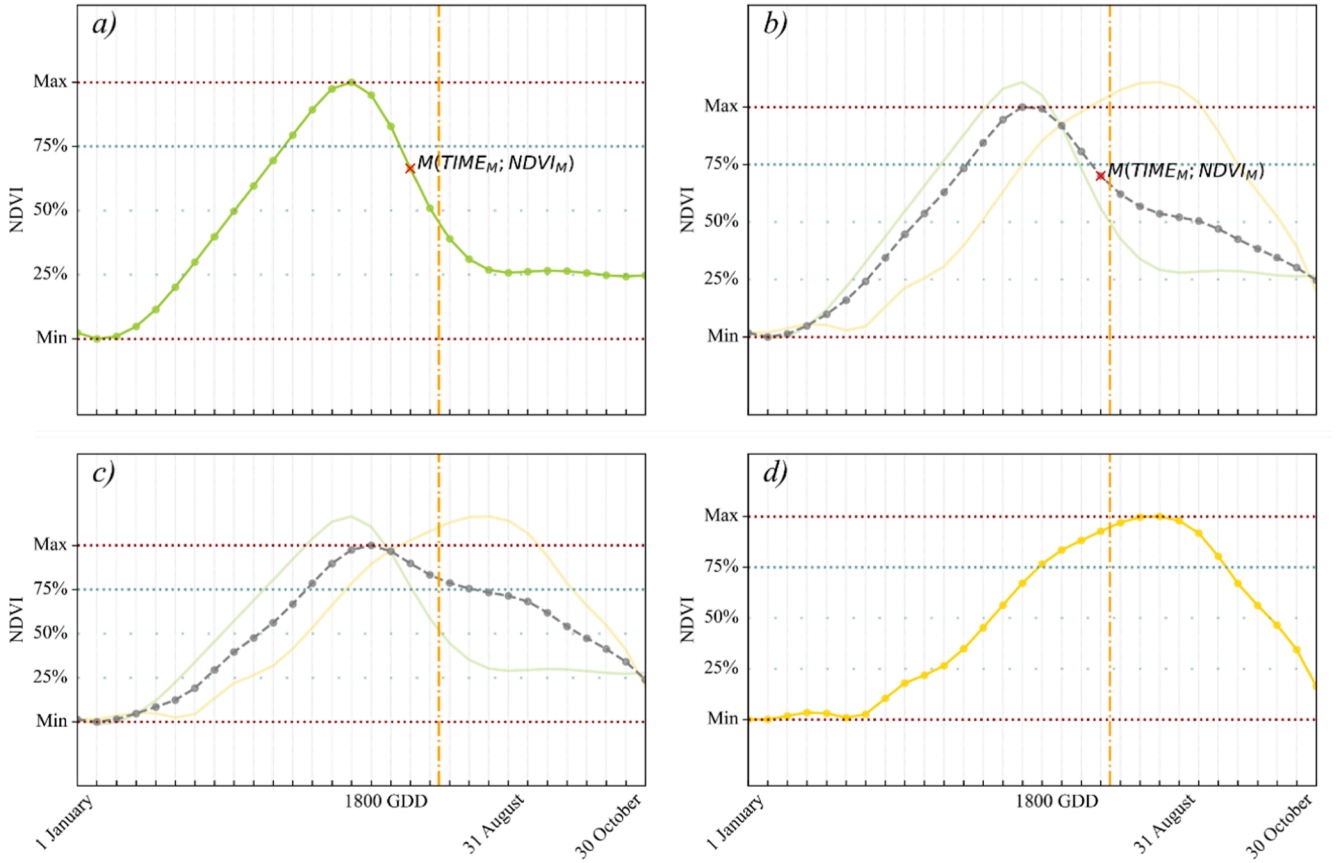

Fig. 2. Example NDVI profiles of arable land pixels with different crop composition: pure winter crop (a); 70% winter crop and 30% summer crop (b); 50% winter crop and 50% summer crop (c); and pure summer crop (d). In (b) and (c) green and yellow lines represent the pure winter and summer crop NDVI profile, respectively, used to infer the linearly-mixed profile (grey). The blue lines correspond to different thresholds on the (compound) NDVI: 75% (dense dots), 50% and 25% (loose dots). The red lines represent the minimum and maximum NDVI of the profile. The vertical line is the date when an accumulation of 1800 GDD occurred; M is the point that identifies the presence of a clear senescence before 1800 GDD and which is used to identify a pixel as winter crop.

The comparison against $AFI_{fodder}90$, and $AFI_{dry\_pulses}90$, the two remaining classes of non-winter crops, is not reported Both approaches to compute winter crop area and winter crop profiles as they accounted for less than 0.2 % of the total number of AFI_{arable_land} pixels.

Temporal consistency was assessed in two ways. First, we compared the annual winter crop area obtained from AFI_{winter_MODIS} maps with the annual winter crop area from official statistics. This comparison was done at country and at EU27 level due to the limited availability of regional statistics of winter crops. The total winter crop area was derived from AFI_{winter_MODIS} maps using a latitude-corrected approximation of each pixel's area. The quantitative assessment was done using the mean absolute percentage error (MAPE):

$$MAPE_r = \frac{1}{n}\sum_{i=1}^{n}\left|\frac{Area_{\mathrm{AFIwinter\_MODIS}_{i,r}} - Area_{\mathrm{EUROSTAT}_{i,r}}}{Area_{\mathrm{EUROSTAT}_{i,r}}}\right| * 100 \quad (1)$$

where r is the considered region, n is the total number of years and i is a given year for which the winter crop area from statistics ($Area_{EUROSTAT}$) and from AFI_{winter_MODIS} ($Area_{AFIwinter\_MODIS}$) is compared.

Second, we visually compared the inter-annual behaviour of the regional NDVI profiles derived from all computed AFI maps (i.e., AFI_{winter_MODIS} and the EU2018-derived AFIs). We qualitatively assessed if the regional NDVI profile from AFI_{winter_MODIS} corresponded to an expected winter crop phenological cycle and to what extent it matched the regional NDVI profile extracted by the AFIs. Regional NDVI values for each AFI were computed using a weighted mean of the pixels in the region, with the share of crop or arable land contained in each pixel as the weight (Genovese et al., 2001). Both approaches to compute winter crop area and winter crop profiles have the advantage to down-weigh those pixels with lower winter crop presence and where more confusion could occur with other land covers present in the pixels (e.g., grassland).

2.3.2. Annual winter crop maps to describe crop yield

To assess if the use of the annual MODIS winter crop maps can better describe crop yield interannual variability, we performed linear regression between timeseries of soft wheat yields and regionally-aggregated NDVI from the annual AFI_{winter_MODIS} maps. The goodness of fit resulting from this analysis was compared with that obtained using NDVI aggregated with three static maps from EU2018 (i.e., AFI_{arable_land}, AFI_{winter_crop}, AFI_{soft_wheat}).

Per administrative region (i.e., NUTS) and year, we spatially aggregated 10-day NDVI values for 2002–2020 using the static EU2018-based AFIs, applied to the whole timeseries, as well as the annually-varying AFI_{winter_MODIS} for each corresponding year. Then, we used the approach of López-Lozano et al. (2015) to determine the best time period for NDVI accumulation. That is, we summed all possible combinations of consecutive 10-day NDVI values from 1 January to 31 August, for a total of 300 combinations. Each combination of aggregated NDVI timeseries (e.g., 1 January-10 January or 1 January-20 June) was used separately in a linear regression model, to describe the temporal yield variability of soft wheat at NUTS level. For each spatial aggregator (i.e., AFI_{winter_MODIS} AFI_{arable_land}, AFI_{winter_crop}, and AFI_{soft_wheat}) we retained the predictor that attained the highest R^2, and also calculated the associated significance value and RMSE (root mean square error). To evaluate if the use of our annual MODIS-derived maps better describes crop yield interannual variability, we compared the performance of models based on AFI_{winter_MODIS} ($models_{winter\_MODIS}$) with models based on AFI_{winter_crop} and AFI_{arable_land} ($models_{winter\_crop}$ and $models_{arable\_land}$).

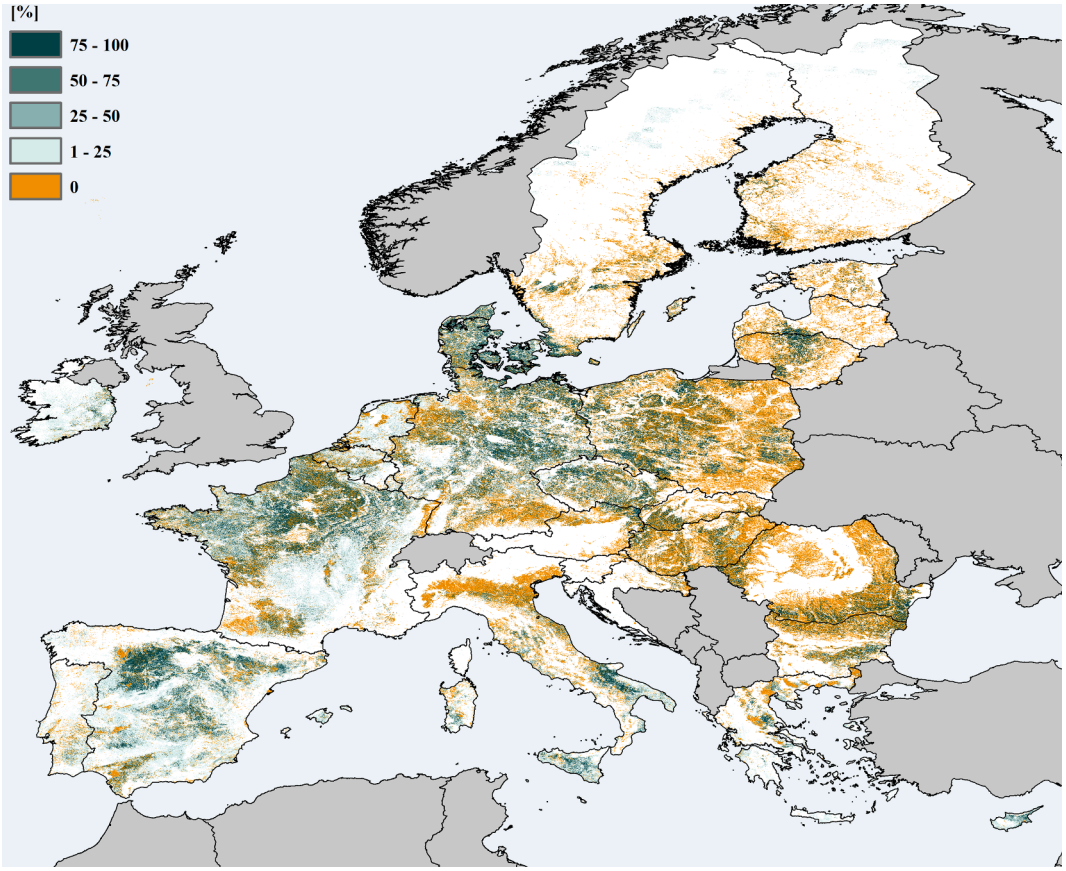

Fig. 3. Winter crop distribution in the EU27 countries for 2018 (AFI_{winter_MODIS}). Green colours indicate pixels that have a dominant winter crop signal. Darker green colours indicate pixels with a higher proportion of arable land. Orange pixels are arable land for which no winter crop presence is detected. White colours show non-arable land areas.

3. Results

3.1. MODIS-based winter crop maps

3.1.1. Spatial analysis

Fig. 3 shows the AFI_{winter_MODIS} map for 2018, as an example. The map correctly identifies areas with a strong density of winter crops. For example, in southern Italy durum wheat and barley winter crops are predominant, and our maps show a majority of pixels detected as winter crops; whereas for northern Italy, where maize and soybean summer crops dominate, fewer pixels are identified as winter crops. Main producing regions for soft wheat, like north-east Germany and northern France, also have high AFI_{winter_MODIS} values. South-eastern Poland has a low AFI_{winter_MODIS}, which corresponds to a dominance of maize in that region.

Table 1 provides a quantitative summary of the validation (AFI_{winter_LPIS} as reference) and the comparison (AFI_{winter_crop} as reference), expressed in terms of area for the selected threshold of 50 %. We observed low omission error (0.17) but higher commission error (0.23), while both producer (0.86) and user (0.77) accuracy are very high for our product AFI_{winter_MODIS}. The comparison against EU2018 presents similar results to the validation with AFI_{winter_LPIS}, but with a higher omission error (0.23), lower commission error (0.17), a similar producer accuracy (0.82), and slightly higher user accuracy (0.83). The comparison of AFI_{winter_crop} against AFI_{winter_LPIS} showed good accuracies and low commission errors (Table S7 – S9) supporting our choice to use EU2018 as a reference for the comparison with our product at continental scale.

We further observed that our commission error with almost pure summer crop pixels ($AFI_{summer\_crop}90$) is low with only 5 % of these pixels classified as winter crop. The misclassification did not follow a specific spatial pattern, and could potentially be caused by misclassifications in EU2018.

We then assessed the difference between AFI_{winter_MODIS} for year 2018 and the AFI_{winter_crop} from EU2018. Visual inspection (examples in Figure S2) shows that AFI_{winter_MODIS} correctly represents the main spatial patterns of winter crop distribution. Fig. 4 shows the difference between the two products. Three observations can be made: *i*) a large fraction of pixels have a very good correspondence between the AFI values (difference < 10 %), *ii*) underestimation (blue colours) is more frequent and intense towards eastern and northern regions of the EU27; *iii*) overestimation (red colours) occurs in southern and western regions.

3.1.2. Temporal analysis

The total winter crop area in EU27, derived from AFI_{winter_MODIS}, is consistently below the reference EUROSTAT area and shows an interannual variability different from the reference data (Fig. 5a). On average, the difference in winter crop area derived from AFI_{winter_MODIS} is about 19 % lower than that reported by EUROSTAT, ranging from approximately 10 % (2015, 2019, 2020) to 25 % lower (2002, 2010, 2011). For the reference year 2018 only, the difference is about −11 % considering AFI_{winter_MODIS} but + 2 % when considering AFI_{winter_crop}. Country-scale analysis reveals differences with years of over- and underestimation depending on the region (Fig. 5b and Figure S3). For example, for France (Fig. 5b), the main soft wheat producer in the EU27, AFI_{winter_MODIS} underestimates winter crop area in 2002 and 2007 but overall has an 11 % MAPE, indicating an accurate area estimation. Other relevant producers have a MAPE below (Spain, Italy, Bulgaria, and Denmark) or around (Germany) 20 %. These countries account, together with France, for more than 50 % of the soft wheat area in the EU27. All these countries also display the lowest interannual variability of winter crop area from AFI_{winter_MODIS} (Figure S3). Larger errors (between 30 % and 40 % MAPE) are found for Poland and Romania, accounting for 22 % of the EU27 soft wheat area. MAPE analysis reveals spatial clusters (Fig. 5c); for example, in southern European countries (Cyprus, Italy, Spain, and Portugal, Figure S3), AFI_{winter_MODIS} overestimates winter crops area. The Netherlands, Belgium, and Ireland present a similar MAPE and area trend based on AFI_{winter_MODIS}, with the largest winter crop areas detected for the same years (2006 and 2018). Notably, the Netherlands' overestimation in 2018 was nearly 70 % for AFI_{winter_MODIS} and 73 % for AFI_{winter_crop}: the EU2018 map also did not properly detect winter crop area for that year. The Baltic countries (Estonia, Latvia, Lithuania) present an increasing trend in detected winter crop area that peaked in 2020, 2017 and 2015. The year with the lowest winter crop area estimation from AFI_{winter_MODIS} is 2002 for most countries.

To illustrate the effect of different crop maps on regional NDVI profiles, Fig. 6 provides representative examples based on different maps, i.e., AFI_{winter_MODIS}, AFI_{winter_wheat}, AFI_{winter_crop}, and AFI_{arable_land}. These examples are generated for the reference year 2018, and the years with minimum and maximum difference in the EU27 winter crop area when compared to EUROSTAT (2002 and 2015 respectively). The regions selected are five main producing regions for winter wheat. In five cases the NDVI profiles are almost identical across all AFIs (i.e., panels *e, g, h, i,* and *k*): in those regions winter crops constitute the predominant crop group, leading to a consistent pixel selection for all AFIs. The NDVI profiles for year 2018 (panels *a, d, j,* and *m*) obtained from the AFI_{arable_land} present later and slower green-up and senescence phases, with lower NDVI values around the seasonal peak, as compared to the other AFIs that behave almost identically. This suggests that winter crops developed earlier compared to the generic arable land profile. Most of the NDVI profiles derived from AFI_{winter_MODIS} for year 2002 and 2015 (panels *b, c, f, l,* and *n*) show an earlier NDVI increase, as can be expected for winter crops, while the profiles from the other AFIs overlap, depicting a more generic arable land profile. We attribute this to crop rotation practices or other changes in land cover composition, which cannot be accounted for by static AFIs. This is evident in the NDVI profiles obtained for region RO411 for 2015 and 2002 (panels *n* and *p*): while the use of AFI_{winter_MODIS} always results in a recognizable NDVI profile of winter crops, the profiles derived from the other maps show late senescence and low NDVI peaks in 2015, and no green-up phase

Table 1
Results of the validation and comparison between AFI_{winter_MODIS} and the two reference AFIs, reported in total area ($\times 10^3$ha). Panel a) reports the total areas ($\times 10^3$ha) of winter crop detected in the validation (yellow cells) and comparison (blue cells) for year 2018, for the AFIs involved using a 50 % fraction threshold. The total area considered is smaller for the LPIS data than for EU2018, resulting in the differences in total AFI areas for the validation and the comparison. Panel b) reports the error and accuracy metrics for validation (yellow cells) and comparison (blue cells) for year 2018, for the AFIs involved.

a) Area ($\times 10^3$ha)	**Validation**				**Comparison**			
	AFI_{winter_MODIS}		**AFI_{winter_LPIS}**		**AFI_{winter_MODIS}**		**AFI_{winter_crop}**	
	10,360		9,322		35,803		36,466	
b) Metrics	**Error**						**Accuracy**	
	Omission		**Commission**				**Producer**	**User**
	Abs. ($\times 10^3$ha)	**Rel.**	**Abs. ($\times 10^3$ha)**	**Rel.**				
Validation (AFI_{winter_LPIS})	1,543	0.17	2,354	0.23			0.86	0.77
Comparison (AFI_{winter_crop})	8,503	0.23	6,027	0.17			0.82	0.83

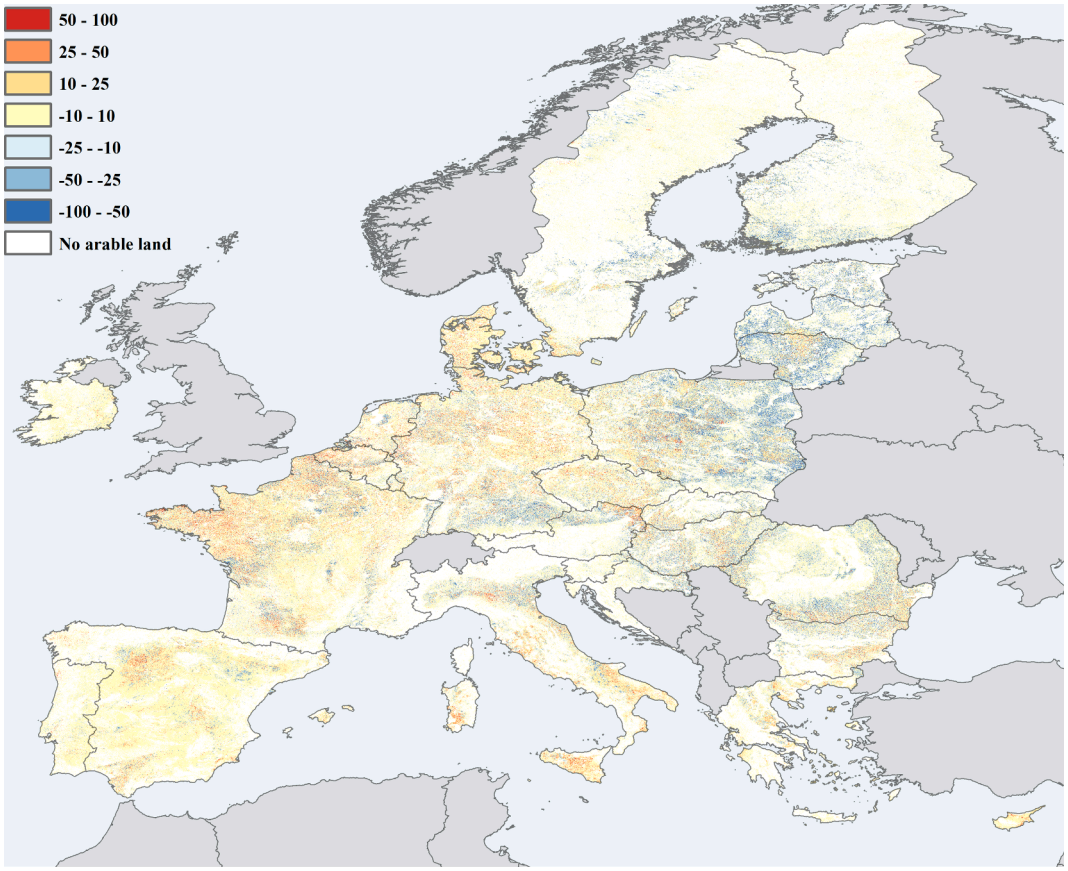

Fig. 4. Difference between AFI_{winter_MODIS} for year 2018 and AFI_{winter_crop}. Blue colours indicate an underestimation ($AFI_{winter\_MODIS} < AFI_{winter\_crop}$), red colours an overestimation ($AFI_{winter\_MODIS} > AFI_{winter\_crop}$), and light-yellow areas denote similar values ($|AFI_{winter\_MODIS} - AFI_{winter\_crop}|<10$ %).

during spring in 2002. Besides the examples in Fig. 6, we observed that, AFI_{winter_MODIS} effectively describes a winter crop phenology. Notably in northern regions (e.g., the Baltic countries, Finland and eastern Poland, Figure S4), the NDVI profiles derived from AFI_{winter_MODIS} show a shorter senescence period compared to the profiles derived from the other AFIs, which lack a distinct senescence phase.

3.2. The use of annual winter crop maps to describe crop yield

Fig. 7 presents the performances of the regional linear models ($models_{winter\_MODIS}$) computed using the timeseries of the accumulated NDVI and soft wheat yield statistics. The highest R^2 values (Fig. 7a) are observed in eastern and northeastern regions and in regions of Germany and Spain. Those regions account for more than 30 % of their respective national production of soft wheat (Table S9). While $models_{winter\_MODIS}$ explain more than half of the yield variance ($R^2 > 0.5$) in 40 % of regions, no to little explanatory power ($R^2 < 0.3$) is observed in 30 % of regions, mostly in western and southern Europe (e.g., France, western Germany, northern Italy). Among the 25 % largest wheat producing regions in the EU27, 13 out of 22 have an average R^2 of 0.2 with mostly no significant models (p-value > 0.05, 8 out of 13) all located in northern France. The remaining nine regions feature R^2 values between 0.5 and 0.7 in five cases and exceeding 0.7 in the other four. The qualitative comparison of the R^2 distribution shows similar results regardless of the base map used for the NDVI aggregation (i.e., AFI_{winter_MODIS} in Fig. 7a; AFI_{arable_land} and AFI_{winter_crops}, in Figure S6). To assess if low R^2 values could result from limited temporal variability in crop yield we regressed the regional-level R^2 values against the corresponding coefficients of variation computed from regional yield timeseries, but this did not result in a significant relationship. $Models_{winter\_MODIS}$ provided $R^2 > 0.5$ for 42 % of the regions (44 % of the average EU27 soft wheat production), compared to 38 % for $models_{winter\_crop}$.

Fig. 7b shows at administrative unit level how the $models_{winter\_MODIS}$ based on the annually-updated AFI_{winter_MODIS} perform with respect to $models_{winter\_crop}$ based on the static AFI_{winter_crops} from 2018. The dominance of light yellow to blue colours indicates that $models_{winter\_MODIS}$ achieved a similar to better R^2 as compared to $models_{winter\_crop}$. While $models_{winter\_MODIS}$ provided better results in large areas of western and northern Europe, worse performances are observed in Greece, western Romania, southern Hungary, and northern Poland. We also found that $models_{winter\_MODIS}$ provided significant models (p-value < 0.05) for 335 regions, 9 % more than that observed using $models_{winter\_crop}$; accounting for 6 % more of the EU27 soft wheat production explained through regression. Our analysis shows that the use of our year-specific winter crop maps overall provides a small, but consistent improvement to crop yield prediction based on linear regression with regionally aggregated NDVI.

4. Discussion

Our study correctly identified 90 % of arable land pixels with dominant winter crop, when compared to EU2018. The resulting maps provide a better description of soft wheat phenology, which improves the crop yield forecasting accuracy when compared to static maps.

4.1. Winter crop maps

The validation against the harmonized LPIS data, performed over 27 % of the EU27 arable land, showed that our method is accurate in mapping winter crop. To further understand the composition of our errors and accuracy we extended the validation exercise to a total of four

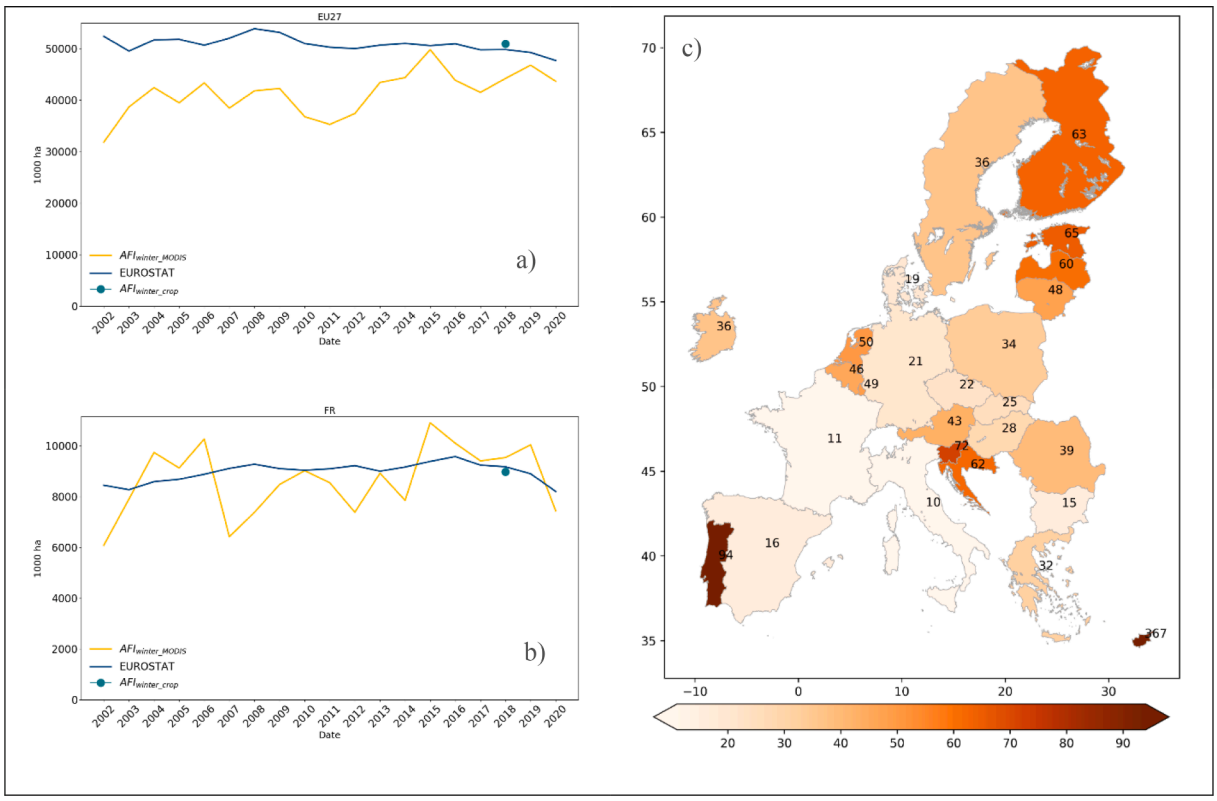

Fig. 5. Timeseries of winter crop area for EU27 (a) and France (b). Timeseries were computed from the annual map obtained with AFI_{winter_MODIS} 2002–2020 (yellow line), from AFI_{winter_crop}(green dot), and from EUROSTAT statistics (blue line). Panel c) displays the country-specific MAPE values.

classes with increasing winter crop coverage (i.e., classes with winter crop share 1–25 %, 25–50 %, 50–75 %, and 75–100 %) and observed that while error and accuracy remained high and almost similar for the first three classes (e.g., omission error 0.58, producer's accuracy 0.42), they drastically improve for the purest class (e.g., omission error 0.19, producer's accuracy: 0.81). This highlights that higher accuracies are obtained for pixels with high winter crop purity.

The comparison between our winter crop map (AFI_{winter_MODIS}) and EU2018 (AFI_{winter_crops}) encompassed all EU27 arable land. The appropriateness of using EU2018 as a reference was proven by its comparison against the LPIS data, resulting in a producer's accuracy between 0.77 and 0.93 and a user's accuracy between 0.90 and of 0.92 (Table S9). Overall, the comparison between AFI_{winter_MODIS} and AFI_{winter_crops} showed an overestimation of winter crop area in Mediterranean regions. There, our algorithm attributes almost all arable land to the winter crop class as most crops share the same season. An example is sunflower that, despite being a summer crop, in Spain presents a winter growing cycle as it is planted in late winter. Conversely, underestimation of winter crop area occurred in all other countries, but mostly in northern and eastern regions where the summer crop area is small. In northern regions this may be caused by the presence of spring varieties of winter cereals (e.g., spring soft wheat), which are usually included in the same statistics as winter crops, but possibly having a later senescence than winter crops and thus not identified by our algorithm. In eastern countries underestimation may be attributed to the fragmentation of arable land composition and smaller farm sizes, which results in mixed pixels containing winter crops, summer crops, and natural vegetation. This is reflected by the average farm sizes that are smaller in eastern countries than in western countries. For example, in 2020, only 0.9 % of Romanian farms had an area > 50 ha while in France this was 46 % (Eurostat, 2022). The underestimation of winter crop area was expected as our approach does not recognize pixels with low crop presence, resulting in a mixed signal (Fig. 1d and Figure S1).

We further observed that the difference in interannual variability observed between winter crop area detected with our algorithm and winter crop area from EUROSTAT statistics (Figure S8) may be influenced by the interannual variability of crop phenology, despite the GDD normalization. For example, in Belgium, Ireland, and the Netherlands, our algorithm detected peaks in winter crop area for 2006 and 2018 (Figure S3). The likely reason for these peaks is the high temperatures experienced during spring and summer of those years leading to earlier grassland mowing and silage maize harvest to prevent wilting. As consequence, the NDVI profiles of winter and summer crops overlapped more, showing a winter crop-like profile with early senescence, thus leading to more winter crop pixels detected in our maps.

Compared to previous crop-group mapping exercises (Weissteiner et al., 2019; Skakun et al., 2017), our approach effectively addresses three limitations:

i) We incorporate more information about crop development (i.e., senescence) relevant for crop yield forecasting, rather than relying on timing of maximum NDVI only. For example, Fig. 2c presents a profile characterised by an equal presence of winter and summer crop; here the timing of maximum NDVI (Weissteiner et al., 2019) would identify a winter crop, whereas the mixed signal becomes clearer in the senescence phase, which we account for.

ii) While Weissteiner et al. (2019)'s method leads to outputs at the end of the agricultural season (e.g., October) our maps can be produced a few weeks after winter crop flowering (e.g., July). Although possibly later than Skakun et al. (2017), this is still well before the end of the agricultural season, which is valuable for operational crop yield forecasting of winter crops.

iii) We classify each arable land pixel using only information associated with the winter crop cycle, while Weissteiner et al. (2019)

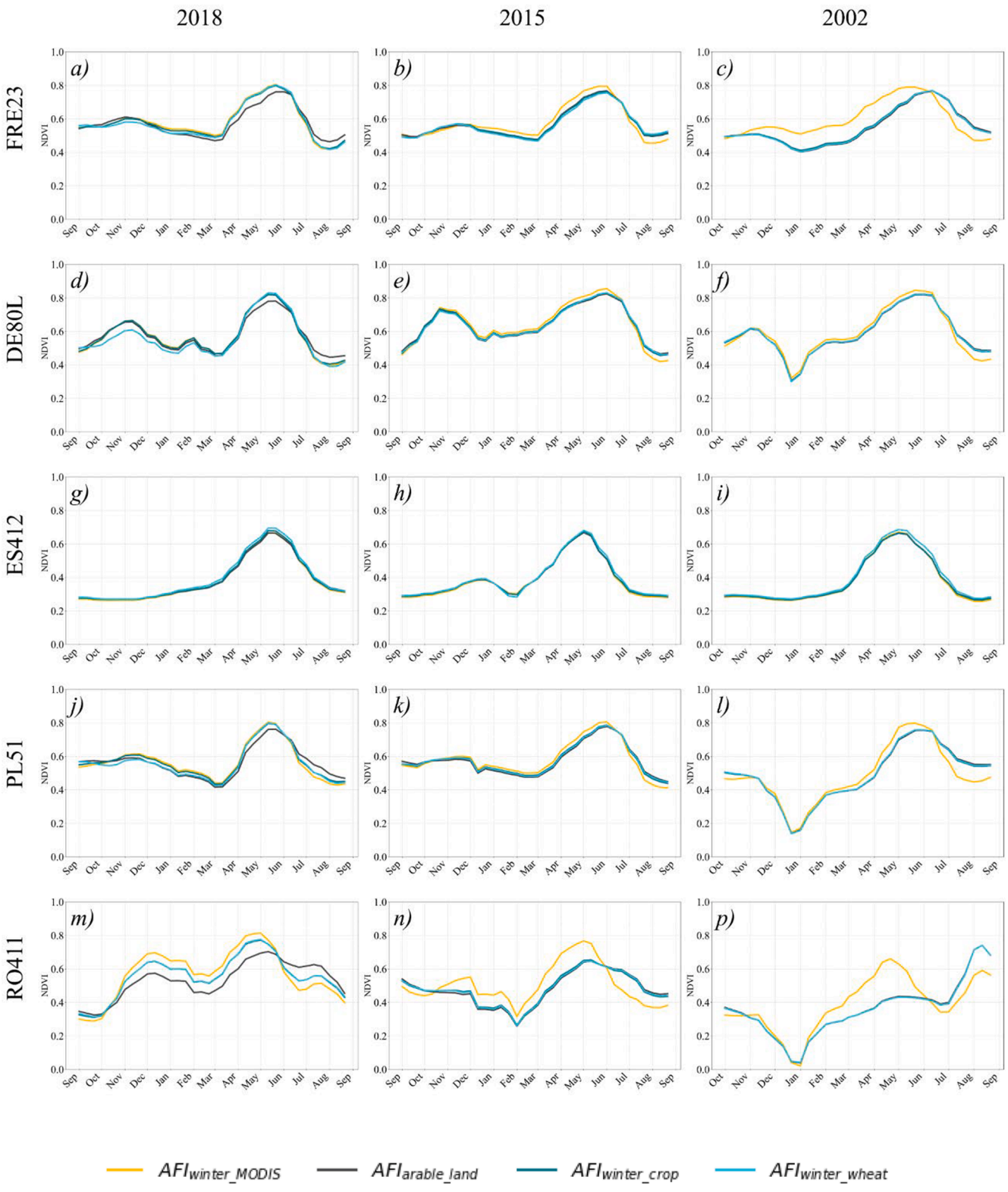

Fig. 6. Regional NDVI profiles computed for the five regions (rows) and three years (columns). Four AFIs are used to extract the signal: AFI_{winter_MODIS} (gold), AFI_{winter_crop} (dark green), AFI_{arable_land} (dark grey), and AFI_{winter_wheat} (light blue). The left column displays the NDVI timeseries for the 2018 agricultural season (1 October – 30 August), the central for 2015 and the right column for 2002.

only classify 11 % of the arable land pixels with the risk of having too few pixels per region, preventing robust statistical analysis.

In addition, our results reported a higher user accuracy when compared to Skakun et al. (2017) (89 % vs 85 %) despite that they used a smaller validation sample (800 pixels vs more than 7 million for our validation) and focussed on Ukraine, where detection of pure winter crop pixels is easier compared to the EU27 because of the larger average farm size, which is 1,000 ha in Ukraine (FAO, 2023) against 17.4 ha for the EU27 (Eurostat, 2022).

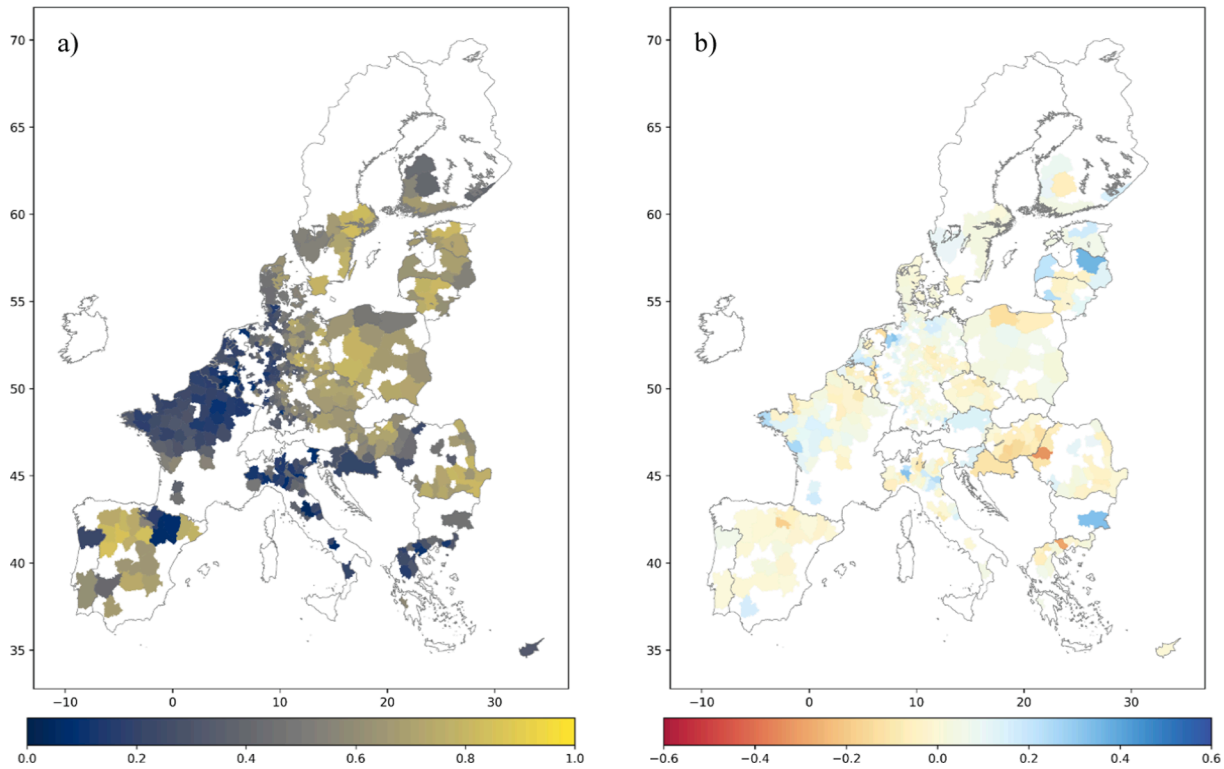

Fig. 7. a) r^2 of the best regression performances obtained at NUTS level with $models_{winter\_MODIS}$, computed for each region, using the associated timeseries of accumulated NDVI values from AFI_{winter_MODIS} aggregation, against the timeseries of soft wheat yields. b) Difference in R^2 between the results from $models_{winter\_MODIS}$ and those obtained from $models_{winter\_crop}$: positive values (blue colours) indicate a better performance of annual $models_{winter\_MODIS}$.

Lastly we observed that the use of a static arable land mask for the entire time series had a minor impact as arable land distribution is relatively static over the years (0.5 % change in total arable land area between 2000 and 2018; European Environment Agency, 2023). However it is necessary to exclude those pixels which have no probability to present winter crop (e.g., fully covered by forest) and to down-weigh for regional average those pixels with low arable land share and thus high probability to have confusion with other vegetation classes, such as grassland, that may have similar phenology with winter crops.

4.2. The use of annual winter crop maps to model crop yield

We demonstrated that spatial aggregation of NDVI for the MODIS-based year-specific maps resulted in a better performance of region-specific yield models for soft wheat, as compared to using a single high-resolution map. While significant error reduction is observed for regions of the Baltics, northern Germany, and Bulgaria, the reduction is smaller when all the EU27 regions are considered (RMSE decreased by 3 %). We observed clear spatial patterns in the explained variance of crop yields with higher R^2 values and predominance of regions with s statistically significant regression (i.e., p-value < 0.05) in southwestern, eastern, northern and northeastern regions.

This pattern is similar to that observed by López-Lozano et al. (2015), who used a static arable land map to extract regional satellite-derived fAPAR (fraction of Absorbed Photosynthetically Active Radiation) timeseries at 1 km resolution and correlated it with yield statistics at sub-national level for the period 1999–2012. Notably, we confirmed that in large areas of western Europe vegetation indexes can only partially explain soft wheat yield variability. Indeed crop yield is not only a function of green biomass (directly associated to NDVI) but of more factors including for example frost or heat stress (Barlow et al., 2015).

Annual maps result in a higher R^2 between aggregated vegetation indexes and yield compared to static maps in large areas of central and northern Europe (Fig. 7b), which confirms the findings by Ronchetti et al. (2023) on soft wheat. We observed this for 56 % (226 over 403) of the regions with significant correlation ($p < 0.05$), whereas Ronchetti et al. (2023) for 37 % (28 over 75). When all the regions are considered, the regression performed between yield and NDVI aggregated with our maps offers a slightly stronger average correlation (0.51 vs 0.45) even though Ronchetti et al. (2023)'s correlation is obtained using the yield time series of the predominant winter crop in each region, and not against soft wheat yield only, as in our case. This suggests that the use of our maps can result in better forecasting outcomes compared to those by Weissteiner et al. (2019), used by Ronchetti et al. (2023).

Despite that the use of AFI_{winter_MODIS} allows to depict a more realistic NDVI winter crop trajectory as compared to those obtained by the two benchmark AFIs (AFI_{winter_crop}, AFI_{arable_land}), this is not always translated into a better description of the soft wheat yield variance. One reason is that the main winter crop cultivated was not soft wheat and thus the winter crop trajectory does not describe soft wheat canopy conditions, such as in northern Spain, where the dominant crop is barley. A second reason is that the selected pixels with winter crops dominance were not representative for winter crops in the region, as in Hungary and its southern bordering regions. In fact, these regions have a limited presence of pixels with winter crop dominance and a large number of pixels with a mix of winter and summer crops (e.g., Fig. 2c). Therefore, the detected winter crop pixels are only those with a distinct early senescence (Figure S5), but may not effectively represent soft wheat phenology, as soft wheat may be predominantly found in mixed pixels. Similarly, both Ronchetti et al. (2023) and López-Lozano et al. (2015) also achieved poor correlations for these Hungarian regions.

4.3. Outlook

Two limitations of the proposed approach limit its use in an operational crop yield forecasting context: the uncertainty in the GDD estimation, and the late timing of mapping. For GDD, we used a fixed season start date (1 January) despite the fact that winter crop sowing dates vary

by year and location, because no accurate information is available on precise location- and year-specific sowing dates for winter crops. To reduce this uncertainty linked to GDD estimation a different approach may use only the GDD requirements for the period flowering-maturity instead of sowing-maturity. Indeed, flowering date is strongly associated with the time of maximum NDVI, and as such easily detectable at pixel level, while the GDD requirements between flowering and maturity are well-known from literature.

With our method the winter crop map can only be derived once a reasonably complete NDVI profile is present (at least until 1800 GDD or 31 August); this limits its use for crop yield forecasting purposes to later stages of the winter crop season The late time of mapping could be improved defining as winter crop those pixels that reach the date of maximum NDVI within the GDD requirements for flowering. Such an approach would provide winter crop maps around the flowering date with a relevant gain for policymakers who aim to have accurate crop yield forecasts well before harvest.

Our study used a simple regression approach to assess whether annual MODIS-derived winter crop maps can be useful for yield prediction. More complex approaches that combine multiple predictors could be applied to further enhance the accuracy of yield forecasts. This could for example be achieved through the use of non-linear approaches, such as machine learning, which besides remotely-sensed vegetation status could also incorporate meteorological data.

Finally our method has the potential to be applied with different remote sensing data and in various geographical settings. Beyond the use of NDVI, the method could equally be implemented with time series of other vegetation indexes and biophysical variables (e.g., the Enhanced Vegetation Index, EVI or the fraction of absorbed photosynthetically active radiation, FPAR) and to sensors or vegetation products with different spatial resolution. For example, we expect a similar accuracy when applying our method to Copernicus timeseries of biophysical parameters (Wolfs et al., 2022) as they are based on Sentinel-3 and Proba-V sensors, with a similar resolution (300 m) as the MODIS data used in this study. If applied to timeseries of vegetation indexes with higher spatial resolution (e.g., Sentinel-2′s 10 m NDVI) the accuracy would likely increase as in that case mostly pure arable land pixels would be present, removing disturbances caused by non-arable land in the mixed pixels, even if the temporal resolution of the data could become problematic in areas/periods with significant cloud cover (Whitcraft et al., 2015). Applying the method to timeseries with coarser spatial resolution (e.g.,MODIS's 500 m FPAR, (Myneni, 2020) would likely yield lower accuracy as winter crop pixels would be more mixed with other land cover types. This may not necessarily have a negative effect when using the resulting maps in crop yield forecasting as our algorithm would still select pixels with winter crops dominance. We would anyhow expect a smaller number of pixels detected with predominance of winter crops, notably in regions where the method is already prone to misdetection (e.g. northeastern EU27). Application in other geographical settings (i.e. outside the EU27) is possible, particularly if winter and summer crops in those settings have similar temporal growth patterns (Hao et al., 2020) as in EU27. Potentially, it may require however a new parametrization of the GDD threshold, adapted to the winter crop varieties dominant in those areas, especially if the regions have substantially different climate characteristics, crop varieties, and season definitions from those in the EU27.

5. Conclusions

This study presented a novel approach using moderate-resolution satellite and temperature data to identify pixels with a dominant winter crop NDVI signal. We used location-specific growing degree day accumulations to identify the annual date of theoretical maturity of a winter crop, and evaluated for each pixel if NDVI displays a clear decrease before that date. Applied to the year 2018 the resulting map showed good correspondence with data from farmers' declaration (LPIS data from Claverie et al., 2024) and with an existing high-resolution crop map for Europe (d'Andrimont et al., 2021). The advantage of our approach over high-resolution crop mapping is its applicability to long historical timeseries, and the generation of consistent annual maps sufficiently early in the season to be of use for yield prediction before the end of the agricultural season. Despite the limited stability in area estimates between the years considered, the annual selection of pixels with dominant winter crop signal positively affected yield forecast accuracy, particularly in eastern, northern, and northeastern European countries. The simple yield modelling presented in this paper serves to demonstrate that annual winter crop maps can provide useful input to yield forecasting.

CRediT authorship contribution statement

Lorenzo Seguini: Writing – original draft, Validation, Software, Methodology, Investigation, Formal analysis, Conceptualization. **Anton Vrieling:** Writing – review & editing, Conceptualization. **Michele Meroni:** Writing – review & editing, Conceptualization. **Andrew Nelson:** Writing – review & editing, Supervision.

Declaration of competing interest

The authors declare that they have no known competing financial interests or personal relationships that could have appeared to influence the work reported in this paper.

Data availability

Data will be made available on request.

Acknowledgments

The authors acknowledge Anja Klisch from BOKU University for the preprocessing of the MODIS timeseries and Martin Claverie from the Joint Research Centre for processing and providing the CHEAP dataset.

Funding

This research was supported by the AGRI4CAST project of the Joint Research Centre of the European Commission.

Appendix A. Supplementary material

Supplementary data to this article can be found online at https://doi.org/10.1016/j.jag.2024.103898.

References

Barlow, K.M., Christy, B.P., O'Leary, G.J., Riffkin, P.A., Nuttall, J.G., 2015. Simulating the impact of extreme heat and frost events on wheat crop production: A review. Field Crops Res. 171, 109–119. https://doi.org/10.1016/j.fcr.2014.11.010.

Ceglar, A., van der Wijngaart, R., de Wit, A., Lecerf, R., Boogaard, H., Seguini, L., van den Berg, M., Toreti, A., Zampieri, M., Fumagalli, D., Baruth, B., 2019. Improving WOFOST model to simulate winter wheat phenology in Europe: Evaluation and effects on yield. Agric. Syst. 168, 168–180. https://doi.org/10.1016/j.agsy.2018.05.002.

Claverie, M., Barriere, V., d'Andrimont, R., Koble, R., Van der Velde, M., 2024. In-season Crop Type Mapping: An accuracy evaluation at European scale using the CHEAP Database. Presented at the EO for agriculture under pressure, ESA-ESRIN Frascati, Italy.

d'Andrimont, R., Verhegghen, A., Lemoine, G., Kempeneers, P., Meroni, M., van der Velde, M., 2021. From parcel to continental scale – A first European crop type map based on Sentinel-1 and LUCAS Copernicus in-situ observations. Remote Sens. Environ. 266, 112708 https://doi.org/10.1016/j.rse.2021.112708.

European Environment Agency, 2023. Land cover and land cover changes in European countries in 2000-2018 — Copernicus Land Monitoring Service [WWW Document]. URL https://land.copernicus.eu/dashboards/clc-clcc-2000-2018 (accessed 8.9.23).

Eurostat, 2022. Farms and farmland in the European Union - statistics [WWW Document]. URL https://ec.europa.eu/eurostat/statistics-explained/index.php?title=Farms_and_farmland_in_the_European_Union_-_statistics (accessed 7.12.23).

Eurostat, 2023. APRO_CPSHR [WWW Document]. URL https://ec.europa.eu/eurostat/databrowser/view/APRO_CPSHR/default/table?lang=en (accessed 2.28.23).
FAO, 2023. Ukraine: Impact of the war on agricultural enterprises. FAO. doi: 10.4060/cc5755en.
Genovese, G., Vignolles, C., Nègre, T., Passera, G., 2001. A methodology for a combined use of normalised difference vegetation index and CORINE land cover data for crop yield monitoring and forecasting. A case study on Spain. https://doi.org/10.1051/agro:2001111 21. doi: 10.1051/agro:2001111.
Hao, P., Di, L., Zhang, C., Guo, L., 2020. Transfer learning for crop classification with Cropland Data Layer data (CDL) as training samples. Sci. Total Environ. 733, 138869 https://doi.org/10.1016/j.scitotenv.2020.138869.
IPAS - FAD - USDA, 2023. Winter Wheat Growth Stage v1 (USAF 557th WW) [WWW Document]. URL https://ipad.fas.usda.gov/cropexplorer/description.aspx?legendid=313&regionid=na (accessed 5.16.23).
Johnson, D.M., 2019. Using the Landsat archive to map crop cover history across the United States. Remote Sens. Environ. 232 https://doi.org/10.1016/j.rse.2019.111286.
Klisch, A., Atzberger, C., 2016. Operational drought monitoring in Kenya using MODIS NDVI time series. Remote Sens. 8, 267. https://doi.org/10.3390/rs8040267.
Knott, C., Snyder, E., Sanford, D.V., Salmeron, M., 2017. Estimating the number of growing degree days needed for key development stages in winter wheat. Dept Plant Soil Sci. Univ. Ky.
Lecerf, R., Ceglar, A., López-Lozano, R., Van Der Velde, M., Baruth, B., 2019. Assessing the information in crop model and meteorological indicators to forecast crop yield over Europe. Agric. Syst. 168, 191–202. https://doi.org/10.1016/j.agsy.2018.03.002.
López-Lozano, R., Duveiller, G., Seguini, L., Meroni, M., García-Condado, S., Hooker, J., Leo, O., Baruth, B., 2015. Towards regional grain yield forecasting with 1km-resolution EO biophysical products: Strengths and limitations at pan-European level. Agric. for. Meteorol. 206, 12–32. https://doi.org/10.1016/j.agrformet.2015.02.021.
McMaster, G.S., 1997. Phenology, development, and growth of the wheat (Triticum Aestivum L.) shoot apex: A review. Adv. Agron. 59, 63–118. https://doi.org/10.1016/S0065-2113(08)60053-X.
Meroni, M., Waldner, F., Seguini, L., Kerdiles, H., Rembold, F., 2021. Yield forecasting with machine learning and small data: What gains for grains? Agric. for. Meteorol. 308–309, 108555 https://doi.org/10.1016/j.agrformet.2021.108555.
Myneni, R., 2020. MODIS Collection 6.1 (C6.1) LAI/FPAR Product User's Guide.
NDAWN, 2023. (North Dakota Agricultural Weather Network (NDAWN) Wheat Growing Degree Days [WWW Document]. URL https://ndawn.ndsu.nodak.edu/help-wheat-growing-degree-days.html (accessed 5.16.23).
Porter, J.R., Gawith, M., 1999. Temperatures and the growth and development of wheat: a review. Eur. J. Agron. 10, 23–36. https://doi.org/10.1016/S1161-0301(98)00047-1.
Preidl, S., Lange, M., Doktor, D., 2020. Introducing APiC for regionalised land cover mapping on the national scale using Sentinel-2A imagery. Remote Sens. Environ. 240, 111673 https://doi.org/10.1016/j.rse.2020.111673.
Ronchetti, G., Nisini Scacchiafichi, L., Seguini, L., Cerrani, I., Van Der Velde, M., n.d. Harmonized European Union subnational crop statistics revealclimate impacts and crop cultivation shifts.
Ronchetti, G., Manfron, G., Weissteiner, C.J., Seguini, L., Nisini Scacchiafichi, L., Panarello, L., Baruth, B., 2023. Remote sensing crop group-specific indicators to support regional yield forecasting in Europe. Comput. Electron. Agric. 205, 107633 https://doi.org/10.1016/j.compag.2023.107633.
Schneider, M., Schelte, T., Schmitz, F., Körner, M., 2023. EuroCrops: The largest harmonized open crop dataset across the European Union. Sci. Data 10, 612. https://doi.org/10.1038/s41597-023-02517-0.
Skakun, S., Franch, B., Vermote, E., Roger, J.-C., Becker-Reshef, I., Justice, C., Kussul, N., 2017. Early season large-area winter crop mapping using MODIS NDVI data, growing degree days information and a Gaussian mixture model. Remote Sens. Environ. 195, 244–258. https://doi.org/10.1016/j.rse.2017.04.026.
Steduto, P., Hsiao, T., Fereres, E., Raes, D. (Eds.), 2012. Crop yield response to water, FAO irrigation and drainage paper. Food and Agriculture Organization of the United Nations, Rome.
Teluguntla, P., Thenkabail, P.S., Oliphant, A., Xiong, J., Gumma, M.K., Congalton, R.G., Yadav, K., Huete, A., 2018. A 30-m landsat-derived cropland extent product of Australia and China using random forest machine learning algorithm on Google Earth Engine cloud computing platform. ISPRS J. Photogramm. Remote Sens. 144, 325–340. https://doi.org/10.1016/j.isprsjprs.2018.07.017.
Tian, H., Huang, N., Niu, Z., Qin, Y., Pei, J., Wang, J., 2019. Mapping winter crops in China with multi-source satellite imagery and phenology-based algorithm. Remote Sens. 11 https://doi.org/10.3390/rs11070820.
Toreti, A., 2014. Gridded Agro-Meteorological Data in Europe.
von Bloh, M., Nóia Júnior, R. de S., Wangerpohl, X., Saltık, A.O., Haller, V., Kaiser, L., Asseng, S., 2023. Machine learning for soybean yield forecasting in Brazil. Agric. For. Meteorol. 341, 109670. doi: 10.1016/j.agrformet.2023.109670.
Wardlow, B.D., Egbert, S.L., Kastens, J.H., 2007. Analysis of time-series MODIS 250 m vegetation index data for crop classification in the U.S. Central Great Plains. Remote Sens. Environ. 108, 290–310. https://doi.org/10.1016/j.rse.2006.11.021.
Weissteiner, C.J., López-Lozano, R., Manfron, G., Duveiller, G., Hooker, J., van der Velde, M., Baruth, B., 2019. A Crop group-specific pure pixel time series for Europe. Remote Sens. 11 https://doi.org/10.3390/rs11222668.
Whitcraft, A.K., Vermote, E.F., Becker-Reshef, I., Justice, C.O., 2015. Cloud cover throughout the agricultural growing season: Impacts on passive optical earth observations. Remote Sens. Environ. 156, 438–447. https://doi.org/10.1016/j.rse.2014.10.009.
Wolfs, D., Verger, A., Van der Goten, R., Sánchez-Zapero, J., 2022. Copernicus Global Land Operations "Vegetation and Energy".
Zhang, Y., Chipanshi, A., Daneshfar, B., Koiter, L., Champagne, C., Davidson, A., Reichert, G., Bédard, F., 2019. Effect of using crop specific masks on earth observation based crop yield forecasting across Canada. Remote Sens. Appl. Soc. Environ. 13, 121–137. https://doi.org/10.1016/j.rsase.2018.10.002.